Low-loss SCF-to-MCF Power Splitter Based on a Biconical Splice Taper

Sijing Liang, John D. Downie, Sergejs Makovejs, Periklis Petropoulos, and Yongmin Jung

***Abstract*—We present a splice-taper-based power splitter which efficiently and evenly distributes optical power from a single core fiber (SCF) into multiple cores of a multicore fiber (MCF). By carefully optimizing the design and implementing precise fabrication control, we achieve a record-low insertion loss of 0.3 dB. We further investigate the impact of MCF core inhomogeneity on power distribution uniformity of SCF-to-MCF power splitters. To relax the stringent requirement for highly homogeneous MCFs in high-performance power splitter fabrication, we propose a macrobending-based post-processing technique that equalizes the power among the cores. This method is experimentally validated, effectively reducing the power variation across MCF cores from 24% to 8% without causing additional loss. These results highlight the versatility and manufacturability of the splice taper approach for making SCF-to-MCF power splitters with high power efficiency and very good distribution uniformity, even in the presence of realistic MCF imperfections.**

***Index Terms*—Fiber optics components, multicore fiber, power splitter, space division multiplexing.**

I. INTRODUCTION

MULTICORE fiber (MCF) technology has been actively explored for next-generation optical networks to overcome the capacity limitations of single core fibers (SCFs), with great potential to reduce cable footprint, power consumption and overall system cost [1]. Commercial deployment of 2-core MCF has commenced in the submarine industry to achieve cable capacities on the order of 1 Pb/s to accommodate the demand for data in the near future. The transition from SCF systems to 2-core MCF systems can leverage most existing technologies developed for SCF systems, by utilizing fan-in/fan-out (FIFO) devices to multiplex/demultiplex spatial channels. However, further scaling of cable capacity demands higher core density (e.g., 4-core), where SCF-oriented technologies become less practical, subsequently requiring various dedicated MCF components [2-6] to establish an efficient and robust MCF ecosystem.

SCF-to-MCF power splitters, capable of distributing optical power from an SCF to multiple cores of an MCF, can replace conventional FIFOs and provide a new approach for pump delivery to MCF amplifiers [7]. Such power splitters allow fewer pump lasers than MCF core counts for implementing MCF amplifiers, improving energy efficiency, reducing device footprint and enhancing cost-effectiveness. In addition, SCF-to-MCF power splitters can be easily integrated into fiber lasers for structured light generation or embedded in fiber-optic sensor networks for multi-point signal detection [8-10].

A number of solutions have been studied to achieve SCF-to-MCF power splitters, including the splice taper method [11-13], multimode interference in polygon-shape-core fibers [14], special multicore photonics crystal fiber design [15], and direct laser writing [16]. Compared to other solutions, the splice taper method removes the need for custom-made fiber designs and the complexity and equipment overhead associated with ultrafast laser inscription, offering significant cost-saving, manufacturability and versatility advantages. However, broad applications of splice-taper-based SCF-to-MCF power splitters have been hindered by two main technical challenges – high insertion loss (IL) and poor power uniformity across MCF cores. While simulations predict very low IL (<0.5 dB) and equal power distribution, previous demonstrations reported a much higher IL (>2 dB) and a substantial power imbalance, with core-to-core power difference exceeding 50% [11-13]. This discrepancy in loss between simulation and experiment is largely attributed to suboptimal taper design and insufficient control in fabrication. The root cause for the commonly observed power imbalance and an effective solution to overcome this technical challenge require further investigation.

In this work, we present a high-performance SCF-to-MCF power splitter based on a meticulously designed and precisely fabricated biconical splice taper. This paper is an extension of our recent work presented in ECOC 2025 [17]. By carefully optimizing the taper parameters and the fabrication process, we obtain what we believe to be a record-low IL of 0.3 dB. According to our simulations, the optimized splice taper design is applicable to various SCF and MCF structures and offers broadband operation, manifesting remarkable flexibility of the splice taper approach. Furthermore, we identify core-to-core inhomogeneity in the MCF as the primary cause for imbalanced power distribution and propose a post-processing technique based on macrobending to address this issue, achieving an improved power imbalance of <10% without introducing additional loss. This post-processing technique

Manuscript received xxxx; revised xxxx; accepted xxxx. The work of Sijing Liang and Periklis Petropoulos was partly supported by the Engineering and Physical Science Research Council under Grant EP/X04047X/1. (*Corresponding author: Sijing Liang*)

Sijing Liang, Periklis Petropoulos and Yongmin Jung are with the Optoelectronics Research Centre, University of Southampton, SO17 1BJ, Southampton, UK (e-mail: s.liang@soton.ac.uk; pp@orc.soton.ac.uk; ymj@orc.soton.ac.uk).

John D. Downie and Sergejs Makovejs are with Corning Incorporated, Corning, NY 14831, USA (e-mail: downiejd@corning.com; makovejss@corning.com).

Color versions of one or more of the figures in this article are available online at http://ieeexplore.ieee.org

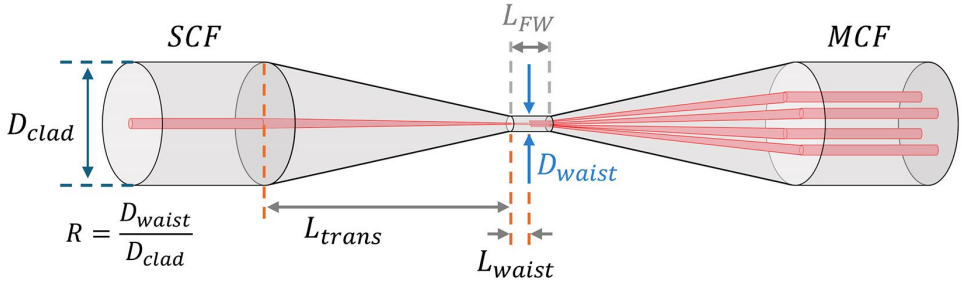

Fig. 1. Schematic of the SCF-to-MCF power splitter based on a biconical splice taper (SCF: single core fiber; MCF: multicore fiber; D_{clad}: cladding diameter; D_{waist}: waist diameter; R: taper ratio; L_{trans}: taper transition length; L_{waist}: taper waist length; L_{FW}: full waist length).

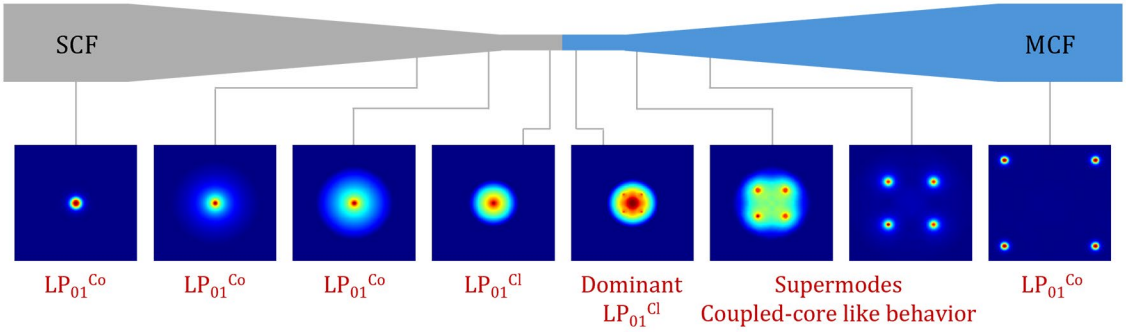

Fig. 2. Calculated transverse field profiles at various positions along the SCF-MCF splice taper (4CF is considered in this illustration example).

effectively reduces the reliance on highly homogeneous MCFs and enhances the practicality and manufacturability of splice-taper-based SCF-to-MCF power splitters for numerous applications.

II. Power Splitter Design and Fabrication

Fig. 1 shows the structure of a splice-taper-based power splitter which has an input SCF, an output MCF and a symmetrical biconical taper centered at the SCF-MCF splice joint. The taper geometry and performance are dictated by three key parameters: taper ratio R of the taper waist diameter to the fiber cladding diameter, taper transition length (L_{trans}), and taper waist length (L_{waist}). SCF and MCF have the same L_{trans} and L_{waist}. The full waist length (L_{FW}) is twice the L_{waist}. The operating principle can be illustrated by the beam mode evolution along the splice taper in Fig. 2. The fundamental LP_{01} core mode (LP_{01}^{Co}) of the SCF is adiabatically transformed into a cladding-guided mode (LP_{01}^{Cl}) in the taper waist. The LP_{01}^{Cl} mode, primarily governed by the cladding/air interface and largely unaffected by the presence of tapered core structures in SCF and MCF, propagates through the splice joint with minimal loss, thanks to the matched cladding diameters of both fibers. In the subsequent up-taper region, the expanding cores of the MCF adiabatically recapture the cladding-guided light, and the LP_{01}^{Cl} mode evolves into a symmetric supermode of the fundamental LP_{01}-like core modes. With a simultaneous increase in core pitch in the up-taper section, the behavior of the tapered MCF changes from coupled core to uncoupled core, resulting in stable and balanced power redistribution across all output cores.

The splice taper approach is applicable to a wide range of MCF designs, e.g., 2-core fiber (2CF), square-lattice 4-core fiber (4CF), and hexagonal-lattice 7-core fiber. In this work, we used the splice taper approach to design and demonstrate an SCF-to-MCF power splitter for a 4CF (Exail, IXF-MC-4-SM-1060). Note that this 4CF has a square-lattice core arrangement with core/cladding diameters of 3.3/125 µm, a core numerical aperture (NA) of 0.21, and a core pitch of 44.2 µm on average. Considering the context of pump delivery for MCF amplifiers, the design wavelength was set to 980 nm. For stable single-mode operation, we selected the Corning HI1060 fiber as the input SCF, with core/cladding diameters of 5.3/125 µm and an NA of 0.14. Smooth linear taper profiles were considered in both our modelling and experiment.

We first optimized our taper design by evaluating the IL of the power splitter as a function of taper parameters (R, L_{trans}, and L_{waist}) using the beam propagation method (BPM). IL is defined as the ratio of the aggregate output power from all the MCF cores to the power launched into the input SCF. Note that the 4CF was assumed to have ideal core homogeneity in our modelling. The results in Fig. 3 suggest that <0.5 dB of IL can be achieved when the taper ratio R is ≤0.25 in conjunction with a transition length L_{trans} of >6 mm. Under these optimized conditions, the core diameters are reduced to <1.35 µm and <0.85 µm, respectively, with the 4CF core pitch contracted to <11.1 µm. While minimal impact of the waist length L_{waist} on the IL was observed in simulations (Fig. 3 (c)), increasing L_{waist} can improve the alignment accuracy and tolerance in the

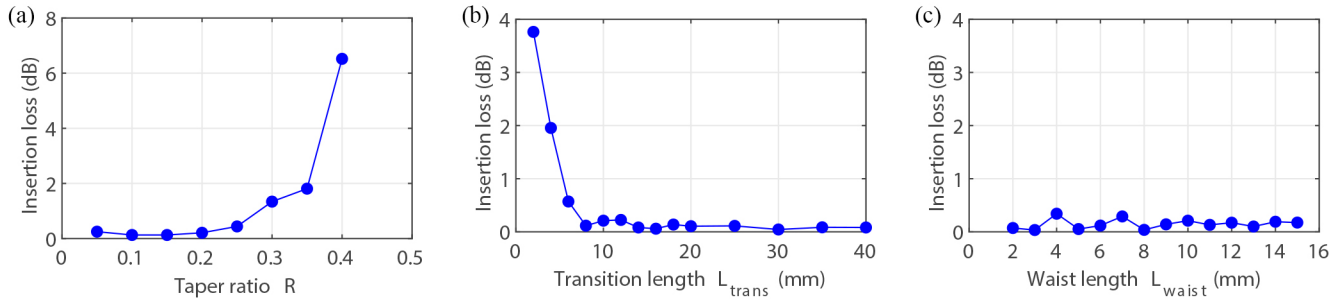

Fig. 3. Calculated IL of the power splitter as a function of (a) taper ratio, (b) transition length and (c) waist length.

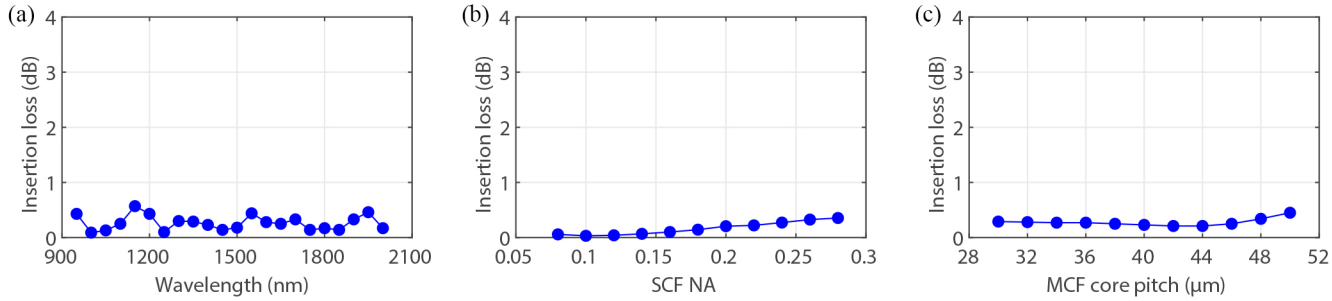

Fig. 4. (a) Operating bandwidth of the SCF-to-4CF power splitter design; calculated IL of the same taper structure (*R=0.2*, L_{trans}*=8 mm*, and L_{waist}*=1 mm*) when different (b) SCF and (c) MCF designs are used, respectively.

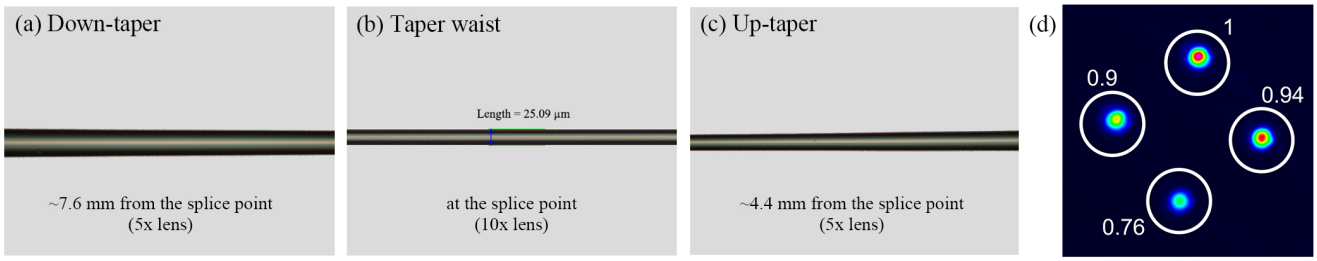

Fig. 5. Microscopic images of the fabricated splice taper taken at different locations showing part of (a) down-taper, (b) taper waist and (c) up-taper regions (background color of images are edited for better contrast); (d) 4CF output beam intensity distribution measured by a CCD camera.

splice taper fabrication. The optical power is always equally divided across the MCF cores.

The operating bandwidth and design flexibility of the splice taper approach were also studied by simulations (Fig. 4). For an SCF-to-4CF power splitter with fixed taper parameters *R*, L_{trans}, and L_{waist}, we calculated the IL across a range of wavelengths, input SCF NA values, and output MCF core pitches. The SCF-to-4CF power splitter can provide low loss operation (<1 dB) over an exceptionally wide bandwidth from 950 nm to 2000 nm. Our simulations in Fig. 4 (b, c) show that the same taper structure remains low loss (<1 dB) for different SCF or MCF designs, because the optimized taper parameters can maintain taper adiabaticity and ensure smooth mode transition in the splice taper at a minimal loss. This avoids the need to optimize critical taper parameters individually for vast combinations of input SCF and output MCF, indicating good design flexibility of the splice taper approach.

In our experiment, we used a Fujikura ARCMaster FSM-100P+ splicer capable of producing precise and replicable adiabatic tapers up to 1:10 in ratio and up to 18 mm in length. This splicer can facilitate the fabrication of low-loss splice tapers by implementing fusion splicing and fiber tapering in a single program to meet the alignment accuracy requirement of positioning the taper waist at the splice joint. We finalized our splice taper design: *R=0.2*, L_{trans}*=8 mm*, and L_{waist}*=1 mm*, with a calculated IL of 0.2 dB. By carefully optimizing arc power, arc time and splicer motor speed, we achieved a precise splice taper with the splice joint accurately tapered down to 25 μm and smooth transitions in the down-/up-taper sections, as shown by the microscopic images in Fig. 5. We used a superluminescent diode centered at 980 nm and an integrating sphere photodiode-based power meter (Thorlabs S145C) to measure the IL as defined. Note that all measurements in this work were taken at 980 nm. The measured IL was only 0.3 dB and in excellent agreement with our simulations. Power imbalance, defined as the difference between the highest and lowest core power, was measured by using a CCD camera to capture the far-field beam image of the 4CF output. In Fig. 5 (d), the normalized core power ratio is 1:0.94:0.9:0.76, yielding a large power imbalance of 24%. This discrepancy

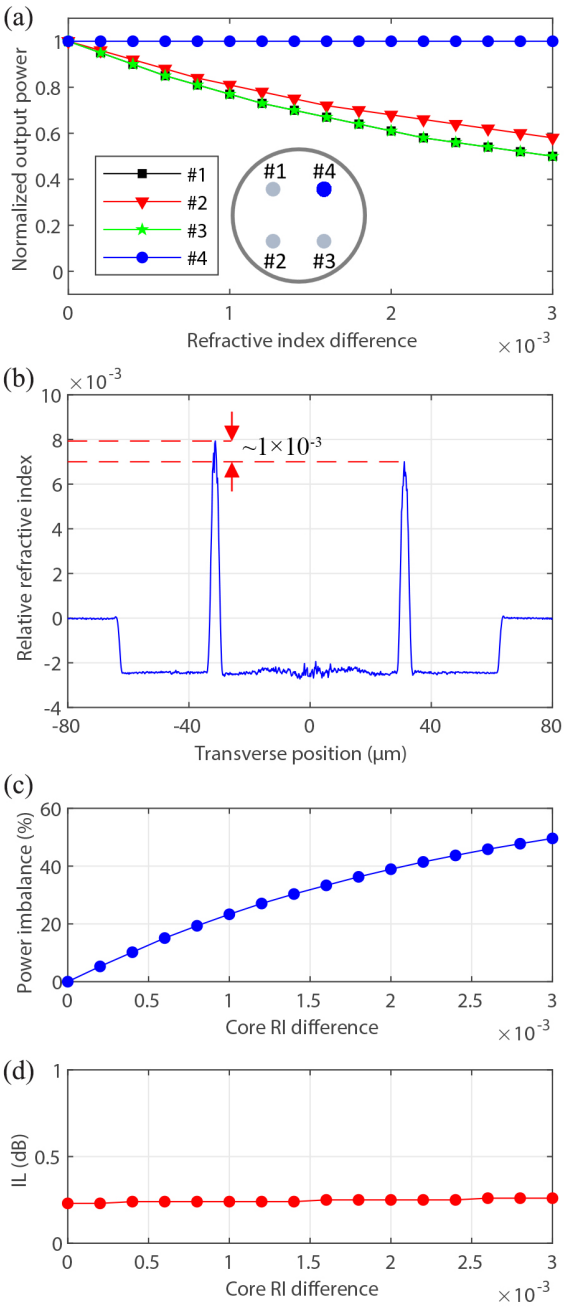

Fig. 6. (a) Simulated impact of RI difference on output power from each MCF core; (b) measured RIP of two diagonal cores of the 4CF; calculated (c) power imbalance and (d) IL as a function of core RI difference.

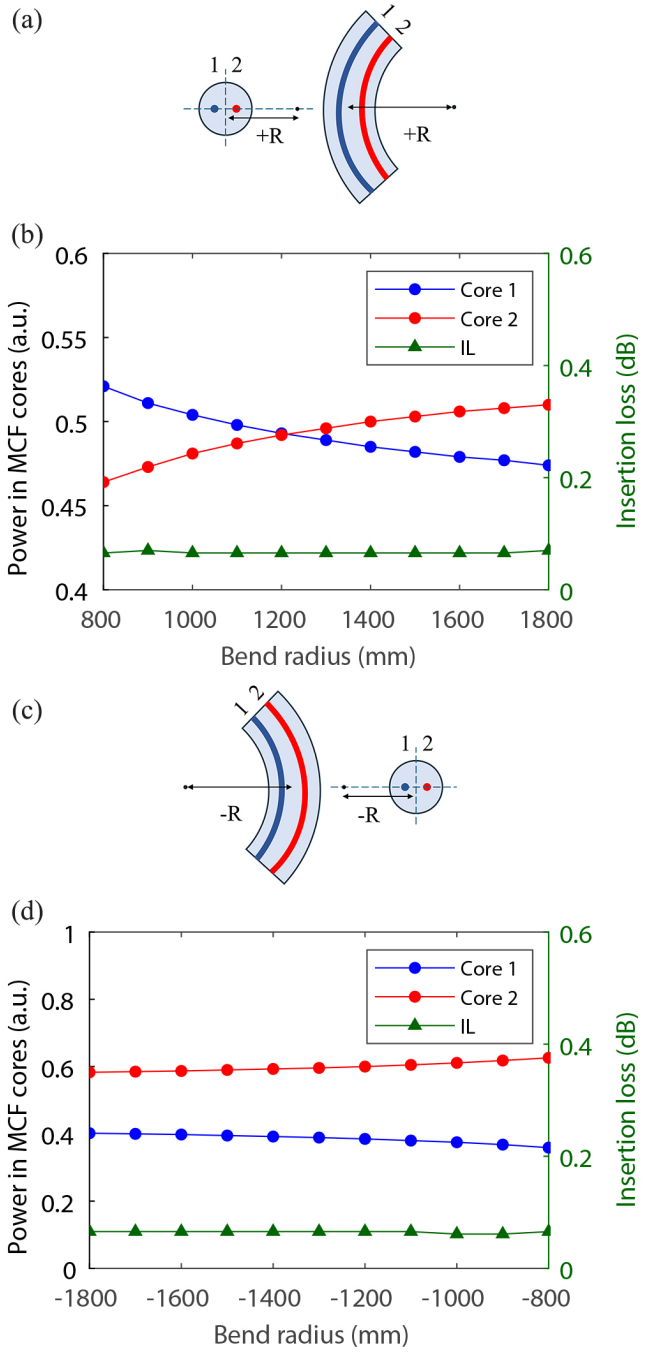

Fig. 7. Simulation results of an SCF-to-2CF power splitter under macrobending effect: (a, c) diagrams illustrating bending direction and bending radius; (b, d) calculated powers in MCF cores and IL of the splice taper as a function of bending radius.

between modelling and experiment results from non-ideal homogeneity in the actual 4CF, such as small variations in core diameter and/or core refractive index (RI).

III. Post-Processing Technique for Improving Core Power Uniformity

We conducted further simulations to study the impact of MCF inhomogeneity on output power distribution in the splice taper. In Fig. 6 (a), we assume a single core (core #4) has a slightly higher RI than the other cores, which share the same RI, while all cores maintain identical diameters. The results indicate an increasing power imbalance with a larger RI difference and core #4 always has the highest output power. The power imbalance reaches ~25% even for a small absolute core RI difference of 1×10^{-3}. This observation aligns well with our measurement of the refractive index profile (RIP) of two diagonal cores in Fig. 6 (b). The power imbalance induced by core RI variation is summarized in Fig. 6 (c). Similar trends

are observed when MCF core diameters are different, e.g., a calculated power imbalance of ~20% for 0.1-μm difference in core diameter. While these MCF core inhomogeneities have a negligible impact on IL (Fig. 6(d)), they significantly degrade power uniformity, undermining the performance and application of splice-taper-based SCF-to-MCF power splitters.

To mitigate the requirement for highly homogeneous MCF in fabrication and enhance the applicability of the splice taper approach, we introduced a post-processing method based on macrobending. This method leverages the sensitivity of each core's effective RI to controlled bending, thereby altering the modal distribution and supermode transitions in the splice taper [18]. To illustrate the feasibility of this post-processing technique, we simulated the performance of a simple SCF-to-2CF power splitter in the presence of macrobending along the entire tapered section (i.e., both taper transition regions and the full taper waist), while excluding the untapered SCF and MCF sections. In this simulation, core 2 was assumed to have a higher RI. The bending strength was characterized by the bending radius and the '+/-' signs represent the two different bending directions (along the X axis) as defined in the diagrams in Fig. 7 (a, c). The results in Fig. 7 (b, d) show how the output powers in the two cores and the ILs of the SCF-to-2CF power splitter vary with the bending conditions. When the bending radius and direction were optimized (R ≈ 1200 mm), the powers in cores 1 and 2 were equalized with no IL deterioration. For a 4-core configuration, when the diagonal core pair (cores 1 and 3) lies along the Y axis (perpendicular to bending along the X axis), the optimized macrobending has only a negligible impact on their output powers (~1% of change relative to the unbent case in simulation), while the dominant power redistribution occurs for the cores aligned with the bending axis (cores 2 and 4). More generally, the 2D macrobending (along X and Y axes) provides two degrees of freedom (DoFs) for power tuning. This is sufficient to equalize 2-core and 3-core structures under arbitrary core inhomogeneity, whereas for N >3 it can still reshape the power distribution but cannot, by itself, guarantee full equalization across all cores unless additional core symmetry (or additional control DoFs) is available. These trends are consistent with established models describing bending-induced effective refractive index perturbations leading to inter-core coupling in MCFs [18-20].

A post-processing platform for splice tapers was developed in-house, as shown in Fig. 8 (a), offering fine tuning of the bending conditions and packaging capability. The fabricated splice taper was loaded on the fiber rotators mounted on 3-axis translation stages which allow precise control of macrobending through X/Y displacement. The output power distribution was monitored in real time by using a laser diode source and a CCD camera. A taper holder (a glass slide in our demonstration) was held near the splice taper ready for packaging. Enabled by our post-processing platform, we optimized the bending conditions applied to our SCF-to-4CF splice taper, reducing the power imbalance from 24% to 8%. The splice taper was subsequently packaged with the optimized bend geometry fixed inside a protective case to ensure long-term mechanical stability. Fig. 8 (b) shows a diagram of the package design. Secured onto a glass slide by UV-cured polymer, the splice taper was raised and suspended in air to ensure low-loss operation. IL remained the same at 0.3 dB after packaging. Measurements repeated after six months showed no degradation. The packaged device (Fig. 8 (c)) has a size of 90×16×13 mm and its output beam profile (Fig. 8 (d)) reveals a normalized core power ratio of 1:1:0.94:0.92. We observed no temperature-dependent behavior of the packaged device on loss and power splitting ratio, even when used in a multicore EDFA with >1 W of total pump power [7].

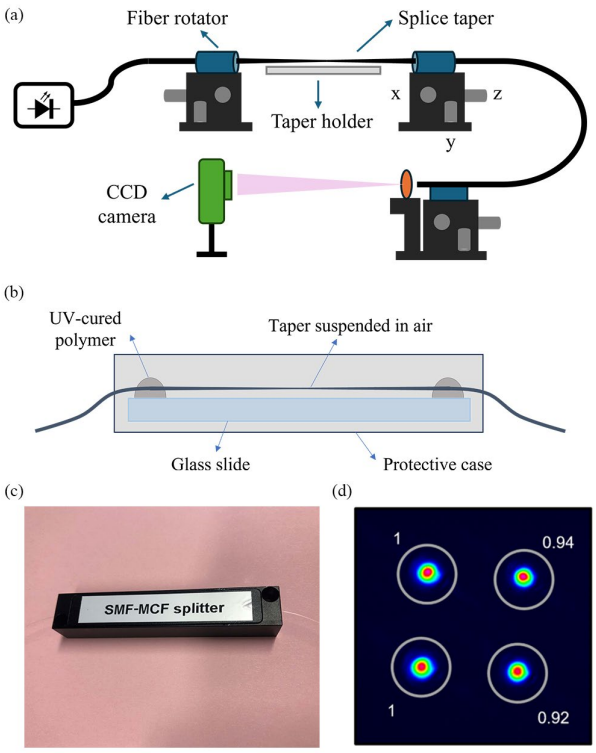

Fig. 8. (a) Schematic of our post-processing platform; (b) diagram of the package design; (c) photo of the packaged SCF-to-4CF power splitter; (d) improved core power uniformity after post-processing.

IV. Conclusion

We successfully designed and demonstrated an SCF-to-MCF power splitter based on the splice taper method. By using an optimized splice taper design and high-precision fabrication, we obtained 0.3 dB of insertion loss – the lowest ever reported to the best of our knowledge. To address the poor core power uniformity issue caused by MCF core inhomogeneity, we also developed a post-processing technique that employs a macrobending effect to readjust output power distribution without incurring additional loss, achieving <10% of core-to-core power variance. This post-processing method relaxes the strict homogeneity

requirements of MCFs, thereby improving significantly the practicality and scalability of splice-taper-based SCF-to-MCF power splitters for diverse applications.

ACKNOWLEDGEMENT

The data for this work is accessible through the University of Southampton Institutional Research Repository DOI: 10.5258/SOTON/D3877.

REFERENCES

[1] J. D. Downie, Y. Jung, S. Makovejs, M. P. Edwards and D. J. Richardson, "Cable Capacity and Cost/Bit Modeling of Submarine MCF Systems With MC-EDFA Alternatives," *J. Lightw. Technol.*, vol. 41, no. 11, pp. 3559-3566, Jun., 2023, doi: 10.1109/JLT.2023.3253259.

[2] V. I. Kopp, J. Park, J. Singer, D. Neugroschl, T. Suganuma, T. Hasegawa, T. Ohtsuka and H. Tazawa, "Ultra-Low-Loss MCF Fanouts for Submarine SDM Applications," in *Proc. Opt. Fiber Commun. Conf.*, 2022, Art. no. Th1E.2.

[3] Y. Jung, S. Alam, Y. Sasaki and D. J. Richardson, "Compact 32-Core Multicore Fibre Isolator for High-Density Spatial Division Multiplexed Transmission," in *Proc. Eur. Conf. Opt. Commun.*, 2016, Art. no. W2B.4.

[4] Y. Jung, S. Alam, D. J. Richardson, S. Ramachandran and K. S. Abedin, "Multicore and multimode optical amplifiers for space division multiplexing," in *Optical Fiber Telecommunications VII*, Academic Press, USA, 2020, ch.7, sec. 2, pp. 305-309, doi: https://doi.org/10.1016/B978-0-12-816502-7.00008-7.

[5] Y. Wakayama, H. Takahashi, N. Yoshikane and T. Tsuritani, "Core-selective Variable-ratio Coupler for Multicore Fiber Applications," in *Proc. Eur. Conf. Opt. Commun.*, 2023, Art. no. We.C.3.4.

[6] Y. Wakayama, N. Yoshikane and T. Tsuritani, "FIFO-less Core-pumped Multicore Fibre Amplifier with Fibre Bragg Grating based Gain Flattening Filter," in *Proc. Eur. Conf. Opt. Commun.*, 2022, Art. no. Th2A.5.

[7] S. Liang, J. D. Downie, S. Makovejs, I. A. Davidson, N. Choudhury, Z. Kakaei, J. Sahu, P. Petropoulos and Y. Jung, "Novel Core-pumped Multicore Fiber Amplifier Integrated with Energy-efficient Pump Light Distributor," in *Proc. Opt. Fiber Commun. Conf.,* 2025, Art. no. W4J.4.

[8] Y. Jung, N. Vukovic, C. A. Codemard and M. N. Zervas, "Multispot fiber lasers for material processing applications," in *Proc. SPIE*, vol. 12865, pp. 56-60, 2024.

[9] Y. Jung, N. Vukovic, C. A. Codemard and M. N. Zervas, "High-efficiency multi-spot beam generation with an all-fiber SMF-SCF structure," *Opt. Express*, vol. 33, no. 10, pp. 21951-21960, May, 2025, doi: 10.1364/OE.554649.

[10] Z. Zhang, A. Rahman, J. Fiebrandt, Y. Wang, K. Sun, J. Luo, K. Madhav and M.M. Roth, "Fiber Vector Sensor Based on Multimode Interference and Image Tapping", *Sensors*, vol. 19, no. 2, 321, Jan., 2019, doi: 10.3390/s19020321.

[11] L. Yuan, Z. Liu and J. Yang, "Coupling characteristics between single-core fiber and multicore fiber", *Opt. Lett.*, vol. 31, no. 22, pp. 3237-3239, Oct., 2006, doi: 10.1364/OL.31.003237.

[12] L. Yuan, Z. Liu, J. Yang and C. Guan, "Bitapered fiber coupling characteristics between single-mode single-core fiber and single-mode multicore fiber," *Appl. Opt.*, vol. 47, no. 18, pp. 3307-3312, Jun., 2008, doi: 10.1364/AO.47.003307.

[13] A. Pytel, M. Napierała, Ł. Szostkiewicz, Ł. Ostrowski, M. Murawski, P. Mergo and T. Nasiłowski, "Optical power 1×7 splitter based on multicore fiber technology", *Opt. Fiber Technol.*, vol. 37, pp. 1-5, Jun., 2017, doi: 10.1016/j.yofte.2017.06.002.

[14] S. Liang, J. D. Downie, S. Makovejs, M. Edwards, P. Petropoulos, and Y. Jung, "Efficient SMF-to-MCF Power Splitter Using Multimode Interference in Square Core Fiber," in *Proc. Opt. Fiber Commun. Conf.*, 2025, Art. no. W4J.2.

[15] S. K. Varshney, K. Saitoh, R. K. Sinha and M. Koshiba, "Coupling Characteristics of Multicore Photonic Crystal Fiber-Based 1 x 4 Power Splitters," *J. Lightw. Technol.*, vol. 27, no. 12, pp. 2062-2068, Jun., 2009, doi: 10.1109/JLT.2008.2006692.

[16] T. Baghdasaryan, K. Vanmol, H. Thienpont, F. Berghmans and J. V. Erps, "Ultracompact 3D splitter for Single-Core to Multi-Core Optical Fiber Connections Fabricated Through Direct Laser Writing in Polymer", *Laser Photonics Rev.*, vol. 18, no. 11, 2400089, Nov., 2024, doi: 10.1002/lpor.202400089.

[17] S. Liang, J. D. Downie, S. Makovejs, P. Petropoulos, and Y. Jung, "0.3-dB-loss SCF-to-MCF Power Splitter Based on a Biconical Splice Taper," in *Proc. Eur. Conf. Opt. Commun.*, 2025, Art. no. M.02.01.4.

[18] T. Sakamoto, T. Mori, M. Wada, T. Yamamoto, F. Yamamoto and K. Nakajima, "Fiber Twisting- and Bending-Induced Adiabatic/Nonadiabatic Super-Mode Transition in Coupled Multicore Fiber," *J. Lightw. Technol.*, vol. 34, no. 4, pp. 1228-1237, Feb., 2016, doi:10.1109/JLT.2015.2502260.

[19]Tetsuya Hayashi, Toshiki Taru, Osamu Shimakawa, Takashi Sasaki, and Eisuke Sasaoka, "Design and fabrication of ultra-low crosstalk and low-loss multi-core fiber," *Opt. Express*, vol. 19, no. 17, pp. 16576-16592, Aug., 2011, doi: 10.1364/OE.19.016576.

[20] Sergi García, Mario Ureña, and Ivana Gasulla, "Bending and twisting effects on multicore fiber differential group delay," *Opt. Express*, vol. 27, no. 22, pp. 31290-31298, Oct., 2019, doi: 10.1364/OE.27.031290.